A single-crystal neutron diffraction study of the structure of the high-temperature rotor phase of lithium sulphate

1992 J. Phys.: Condens. Matter 4 1925

(http://iopscience.iop.org/0953-8984/4/8/008)

J. Phys.: Condens. Matter 4 (1992) 1925–1933. Printed in the UK

A single-crystal neutron diffraction study of the structure of the high-temperature rotor phase of lithium sulphate

Raul Kaber†, Leif Nilsson†, Niels Hessel Andersen‡, Arnold Lundén† and John O Thomas§

† Department of Physics, Chalmers University of Technology, S-412 96 Gothenburg, Sweden

‡ Department of Physics, Risø National Laboratory, DK-4000, Roskilde, Denmark

§ Institute of Chemistry, Uppsala University, Box 531, S-751 21 Uppsala, Sweden

Received 9 September 1991, in final form 7 November 1991

Abstract. The ionic distribution in the high-temperature rotor phase of lithium sulphate, Li_2SO_4, has been reinvestigated by single-crystal neutron diffraction at 923 K. Thermal vibrational tensor terms up to the fourth rank are refined to give a better description of the space–time-averaged Li^+ and SO_4^{2-} distributions. The picture of Li^+ mobility that emerges supports well the earlier proposed notion of rapidly reorienting SO_4^{2-} ions which effectively gate the movement of Li^+ ions, i.e. a 'paddle-wheel mechanism'. The mode of transport for the Li^+ ions would appear to be jumps of 3.5–3.7 Å between ≈90% occupied, tetrahedrally distorted 8c sites (at $\frac{1}{4}, \frac{1}{4}, \frac{1}{4}$), into a spherical shell of radius 2.8 Å surrounding each of four adjacent tetrahedrally coordinated SO_4^{2-} ions. Each shell contains, in total, ≈0.2 Li^+ ions. These Li^+ ions can then jump further into one of the six adjacent 8c sites. The Li^+ transport thus occurs in one of the six directions [110], [1$\bar{1}$0], [101] etc, and gives some support to the notion (corroborated by earlier MD simulation) that the pathways are slightly curved, and hence somewhat in excess of 3.5 Å. This agrees well with the value of 3.7 ± 0.4 Å deduced from Raman spectroscopy, and also with diffuse neutron scattering studies which suggest Li^+–Li^+ pair correlation distances of 3.6–3.7 Å.

1. Introduction

The high-temperature phase of lithium sulphate, Li_2SO_4, is one of the best-known and most widely studied of the class of materials generally referred to as solid electrolytes. In its low-temperature phase, Li_2SO_4 is low-symmetric monoclinic, $P2_1/a$ (equivalent to No 14 in the *International Tables for X-ray Crystallography* (1969), with the *b*-axis unique but with glide along the *a*-direction); see also Nord (1973). At 846 K, the structure undergoes a phase transition to a highly symmetric face-centred cubic phase: $Fm3m$ (No 225), with $a = 7.07$ Å at 883 K. This phase then persists up to its melting point at 1133 K (Førland and Krogh-Moe 1957). The high-temperature phase has a remarkably high ionic conductivity (1.46 S cm^{-1} at 923 K), which can be ascribed to the high mobility of the Li^+ ions (Kvist and Lundén 1965). This phase has attracted much attention in recent years as a model example of a rotor phase, with the low- to high-temperature phase

0953-8984/92/081925 + 09 $04.50

transition involving an anomalously high heat of transition of 24.8 kJ mol^{-1} (Dissanayake and Mellander 1986).

The implication of the term 'rotor phase' emerged from a previous neutron powder diffraction study (Nilsson *et al* 1980) which produced only two significant observable reflections. The refined model involved spherically symmetric SO_4^{2-} ions. These constituted the periodic framework of the structure, with the 'molten' component (the Li^+ ions) moving in the space left between the reorienting anions. This picture was supported by results of diffuse neutron scattering studies (Aronsson *et al* 1983): the diffuse scattering was essentially isotropic, and preliminary analyses of the data suggested that it resulted mainly from the correlations involving the rigid sulphate groups. However, the existence of correlations which also involved the lithium ions was also inferred. Thus, a type of cooperative gating mechanism can be envisaged where Li^+ ions jump and oxygen atoms move around the 'fixed' S atoms of the sulphate ions in a mutually coupled manner. The notion of a 'paddle-wheel'-type mechanism thus emerges whereby the Li^+ ion motion is implicitly coupled to the reorientational motion of the translationally immobile counterions. The fact that a conventional crystallographic description of the structure necessarily involves formally fully occupied sites [at (0, 0, 0) and $(\frac{1}{4}, \frac{1}{4}, \frac{1}{4})$] further reinforces this picture.

The most unsatisfactory aspect of the earlier neutron powder result, however, is that it is based on a model refined from so few neutron observations, and is therefore of little more than qualitative value. In view of this, our term 'paddle-wheel mechanism' has perhaps been interpreted too literally, e.g. Secco (1988a, b), Lundén (1988a, b), Lundén and Dissanayake (1991). The phrase was coined merely to help visualize a complex mechanism whose essential feature is an intimate coupling between SO_4^{2-} rotations and Li^+ jumps. In the present work, the availability of a large single crystal has created a real possibility of refining a considerably more detailed model for the Li^+ and SO_4^{2-} distributions, and thus acquiring a more sophisticated picture of the Li^+ transport mechanism.

2. Experimental details

The lithium sulphate single crystal used in this study was grown *in situ* from the melt in a furnace mounted on the goniometer of a neutron spectrometer. It was essential that the crystal, once grown, should not be allowed to cool into its low-temperature phase below 848 K (Førland and Krogh-Moe 1957; Schroeder *et al* 1972), since the crystal would be destroyed due to the large volume change at the phase transition: 3.2% as determined by x-ray diffraction methods, and somewhat larger from dilatometric studies; while the volume change at the melting point is much smaller (Mellander and Nilsson 1983). Stringent demands were made on the crystal container: it had to resist the extremely corrosive sulphate melt, endure the strains incurred during several attempts to melt and recrystallize the Li_2SO_4, and give a minimal amount of background neutron scattering. It also had to hold a vacuum. Several encapsulation materials were tested unsuccessfully, including electrolytically gold-plated stainless steel, quartz and pyrolitic graphite. All either corroded within a few hours, or cracked when the melt solidified. Success was finally achieved with a container made entirely from 0.5 mm platinum sheet shaped into a 70 mm long cylinder with an internal diameter of 12 mm. The lower end of the container was cone-shaped with an angle of 45°. The top end was provided with a thick platinum collar carrying an internal thread for a platinum end-cap. The vacuum

seal was a soft annealed platinum ring. The pointed end of the lower cone fitted into a 5 mm diameter support bar fixed into the bottom of the furnace.

Isotope enriched Li_2SO_4 (>98.4% ^7Li) was obtained from Oak Ridge National Laboratory. It was carefully dried at 470 K for 48 h and then melted. After crystallization, it was ground and loaded into the platinum container, which was then sealed and mounted in the spectrometer furnace. A cromel–alumel thermocouple mounted on the surface of the specimen can monitor the temperature. Heating was provided by a cylindrical vacuum furnace with a tantalum heating element. The position of the sample holder was adjusted so that the temperature gradient within the furnace caused crystallization to begin at the conical end of the container. After melting at 1133 K, the temperature was lowered at a rate of 2° per hour. The crystallinity of the resulting specimen was checked crystallographically. This procedure had to be repeated several times, since crystallization often resulted in a number of laminar crystals. The preferred direction of growth was along the [011] direction. A crystal 15 mm long with a diameter of 12 mm was finally obtained. The temperature was maintained at a constant 923 K throughout the data collection.

Diffraction data was collected on the TAS4 triple-axis spectrometer at the Risø National Laboratory, using a collimated neutron beam of wavelength 1.425 Å, and no analyser crystal. The data collection was limited to the zone of reflections bounded by the [100]- and [011]-directions, roughly 20 Bragg reflections were measured by longitudinal $\Omega/2\theta$ scans. No correction was made for the very low absorption occurring in the specimen. In view of the small number of measured reflections, the total intensities, background corrections and standard deviations (σ) could all be calculated by hand, as could the Lorentz correction which multiplies I_{obs} to give F^2_{obs}.

3. Refinements

The crude model obtained from our earlier neutron powder diffraction study (Nilsson *et al* 1980) served as the starting point for the refinement of the new more extended data set. On the basis of essentially two strong and two weak reflections, good agreement had been obtained for a model involving a spherically symmetrized sulphate group situated at the octahedral (0, 0, 0) site, and lithium at the tetrahedral ($\frac{1}{4}, \frac{1}{4}, \frac{1}{4}$) site of a face-centred cubic cell. The structure is drawn schematically in figure 1 to give an impression of the closely packed interlocking nature of the anions and cations. Isotropic temperature factors [$B = 8\pi^2\overline{u^2}$] of 30 and 17 Å^2 were refined for the Li^+ and SO_4^{2-} ions, respectively, where $\overline{u^2}$ is the mean-square vibrational amplitude.

Access to a much larger data set allows us to improve considerably the sophistication of the model. The refinements were made using the full-matrix least-squares program DUPALS (Lundgren 1982), where the function minimized was $\Sigma w(F^2_{obs} - |F_{calc}|^2)^2$; the weight ($w$) is given by $1/\sigma^2(F^2)$.

Having first roughly tested the suitability of the original model, the best compromise between physical meaningfulness and goodness-of-fit was achieved for the model summarized in table 1:

(i) Although various disordered models involving discrete, partially occupied oxygen sites were tested, the sulphate ion is still found to be best represented by a spherical scattering model of the form: $f(SO_4) = f(S) + 4[\sin(kr)/kr]f(O)$, where $k = 4\pi \sin\Theta/\lambda$, and r is the S–O distance fixed, as before, to 1.49 Å. The entire ion is

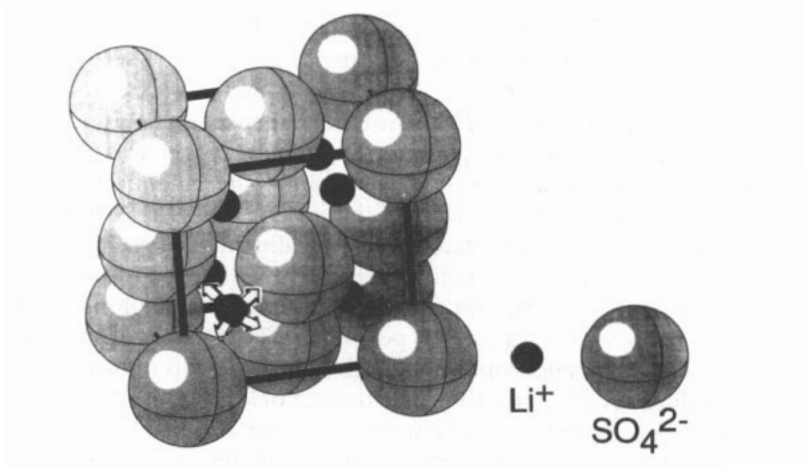

Figure 1. Schematic representation of the cubic high-temperature rotor phase of lithium sulphate. The arrows on the lithium ion at $(\frac{1}{4}, \frac{1}{4}, \frac{1}{4})$ indicate the directions of the tetrahedral distortion of the lithium distribution towards the four neighbouring SO_4^{2-} ions.

Table 1. Final refined model for the high-temperature phase of lithium sulphate at 923 K. (*a*) Fractional coordinates and isotropic mean-square vibrational amplitudes ($\overline{u^2}$). (*b*) Higher rank thermal vibrational tensor terms.

Ionic unit	Occupation	x	y	z	$\overline{u^2}$ (Å^2)
(*a*)					
Li (stat.)	90%	1/4	1/4	1/4	0.25*
Li (mobile)	20%	0	0	0	0.30(4)
'SO_4'	100%	0	0	0	0.11(2)
(*b*)					
Li (stat.)	$\gamma_{123} = -0.004$*				
	$\delta_{1111} = \delta_{2222} = \delta_{3333} = -0.004$*				
	$\delta_{1122} = \delta_{1133} = \delta_{2233} = 0.002$*				
Li (mobile)	$\delta_{1111} = \delta_{2222} = \delta_{3333} = 0.0027(3)$				
	$\delta_{1122} = \delta_{1133} = \delta_{2233} = 0.0015(1)$				
SO_4	$\delta_{1111} = \delta_{2222} = \delta_{3333} = 0.0005(2)$				
	$\delta_{1122} = \delta_{1133} = \delta_{2233} = -0.0003(1)$				

* Thermal model for Li(stat.) fixed in final refinement.

associated with an 'overall' thermal vibrational model involving a combination of isotropic and statistically highly significant fourth-rank vibrational tensor terms (δ_{ijkl}) (*International Tables for X-Ray Crystallography* 1974). We observe from the F_{obs} maps that the apparent oxygen distribution is not spherically symmetric, but is seen to have peaks at $(x, x, 0)$, $(x, -x, 0)$, etc for $x = 0.16$, i.e. 12 positions in all (figure 2(*b*)). This non-spherical oxygen distribution is described in the refined model by the δ_{ijkl} vibrational parameters.

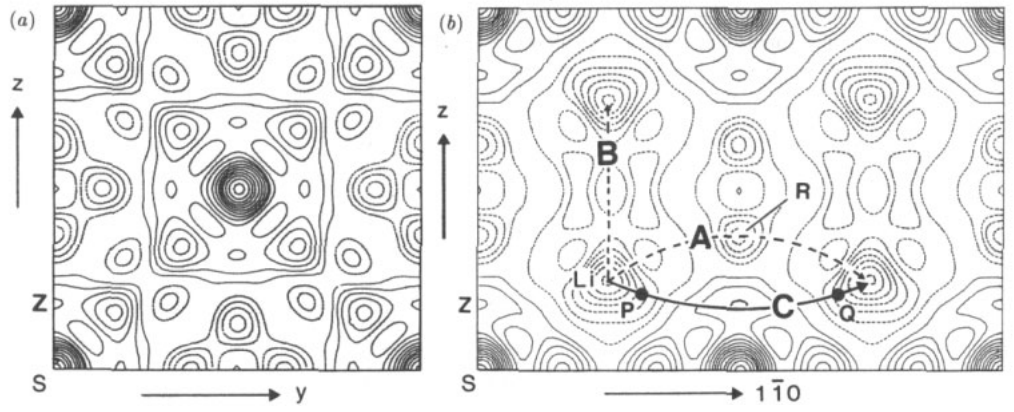

Figure 2. *Observed Fourier synthesis of the nuclear densities in the (a) 100-, and (b) 110-planes. Contours are drawn at the same arbitrary intervals in both sections, and the zero-level contour is omitted. Three possible lithium conduction pathways (A, B and C) are indicated.*

(ii) The refined model for the lithium ions is even more complex: 90% of the ions are located at their earlier tetrahedral 8c ($\frac{1}{4}$, $\frac{1}{4}$, $\frac{1}{4}$)-sites, and carry an isotropic and highly significant non-centrosymmetric third-rank anharmonic vibrational tensor terms (γ_{ijk}). As can be seen from figure 2(*b*), the lithium distribution is significantly tetrahedrally distorted in the directions of its four neighbouring SO_4^{2-} ions. The remaining 10% of the ^{7}Li nuclei are refined as an evenly distributed spherical shell surrounding the sulphate ions, on a sphere of radius 2.8 Å, with its centre at (0, 0, 0). This distance corresponds to that from the origin to the nearest Li^+ sites displaced from ($\frac{1}{4}$, $\frac{1}{4}$, $\frac{1}{4}$) towards the origin. The Li^+ shell (containing, in total, $0.2Li^+$) is given qualitatively the same vibrational model as the SO_4^{2-} ion with which it is structurally linked through a common origin at (0, 0, 0), but is allowed to refine independently. The effective thermal vibrational amplitude for the Li^+ 'shell' is significantly larger than that for the SO_4^{2-} ion (table 1). High correlation between the various parameters meant that neither the 90%/10% ratio nor the figure 2.8 Å were obtained from a refinement, but rather adjusted iteratively 'by hand' to give optimal agreement. Even the thermal model for the 90% Li^+ component had to be fixed at previously refined values to achieve stability in the final refinement.

The final list of F_{obs} and F_{calc} values is given in table 2. No evidence of significant extinction is seen. The observed Fourier syntheses of the nuclear distributions in the (100) and (110) planes, using phases calculated from the above refined model, are plotted in figure 2. It should be noted that, despite the apparently significant peaks at R (lithium has a negative neutron scattering length), extensive efforts to refine a model involving any degree of lithium occupation at the 24e ($\frac{1}{2}$, $\frac{1}{2}$, $\frac{1}{2} \pm \delta$) site failed totally; as did a model involving a central 4b site (at $\frac{1}{2}$, $\frac{1}{2}$, $\frac{1}{2}$). We are thus forced to conclude that the peaks at R are spurious, resulting from Fourier series truncation effects. Such features are to be expected for Fourier summations involving only a few terms. That the peaks are indeed spurious is further supported by the appearance of the corresponding (F_{obs}–F_{calc}) difference Fourier syntheses given in figures 3(*a*)–(*b*). The featureless character of these maps can be taken as a reliable indication of the validity of the refined model. A negative peak also occurs near R in a calculated Fourier synthesis of the Li^+ model alone

Table 2. Observed (F_o) and calculated (F_c) neutron structure factors after the final refinement of the high-temperature cubic phase of lithium sulphate at 923 K.

h	k	l	F_o	F_c
1	1	1	77.1	76.9
2	0	0	71.7	71.1
0	2	2	28.3	27.8
3	1	1	11.1	11.9
2	2	2	4.9	7.3
4	0	0	1.3	1.9
1	3	3	2.8	5.6
4	2	2	7.8	7.2
3	3	3	27.0	25.0
5	1	1	20.1	20.1
0	4	4	4.2	5.4
2	4	4	18.4	18.5
6	0	0	21.1	20.6
5	3	3	13.0	13.9
6	2	2	8.8	5.9
4	4	4	8.0	8.2
1	5	5	3.2	2.2
7	1	1	5.4	6.0

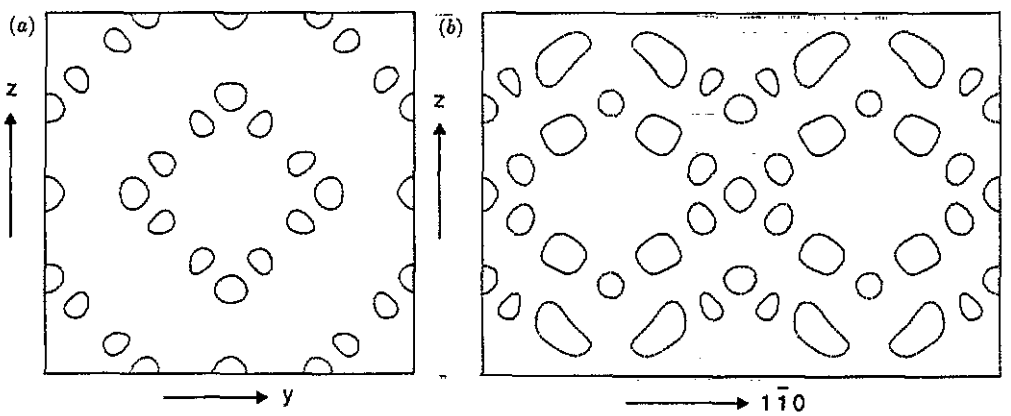

Figure 3. Difference Fourier syntheses corresponding to the nuclear density plots given in figure 2; the contour intervals are 20% of those used in figure 2. The zero-level contour is omitted.

(figure 4), in which no scattering centre is sited anywhere in the vicinity of R. The void at and near $(\frac{1}{2}, \frac{1}{2}, \frac{1}{2})$ must therefore be regarded as experimentally well established. The final agreement factors $R(F)$ and $R(F^2)$ were 5.2% and 3.0%, respectively.

In this connection, it is interesting to note the essential difference compared to the simple fluorite or anti-fluorite cases, where the majority-ion distorts towards the empty region (around $[\frac{1}{2}, \frac{1}{2}, \frac{1}{2}]$), cf. Bachmann & Schulz (1984). It is important to reflect, however, on the essential difference in the fundamental nature of Li_2SO_4 and these other systems: Li_2SO_4 involves a non-centrosymmetric anion at a crystallographic inversion

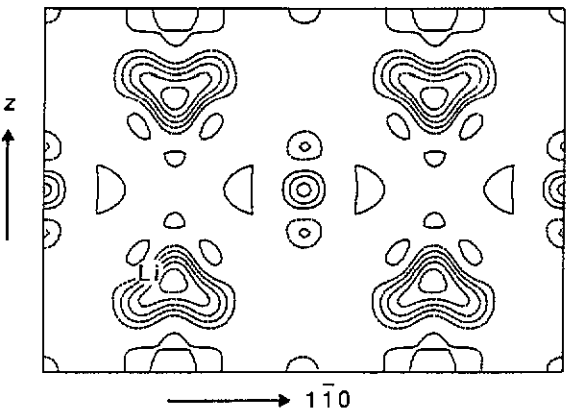

Figure 4. Calculated Fourier synthesis for the lithium distribution alone in the 110-plane; same arbitrary contour intervals are used as in figure 2.

centre. This is the very essence of the proposed 'paddle-wheel' mechanism, and is a feature totally absent in the simple fluorites and anti-fluorites.

4. Discussion

The earlier notion of a 'paddle-wheel'-type mechanism for the movement of Li^+ ions in the HT phase of lithium sulphate envisages a state of dynamical interaction between Li^+ ions and rotating sulphate groups, with the clear implication that the translational movement of the lithium ions is intimately coupled to the reorientation of the sulphate ions. The distance of closest approach between lithium ions and the sulphate oxygen atoms distributed over the surface of a sphere is only 1.57 Å, while the radial sum $[r(Li^+) + r(O)]$ is as large as 1.90 Å.

Because the lithium positions are formally almost fully occupied (90% occupation in the model, in contrast to the implicitly disordered SO_4^{2-} oxygen positions), some form of highly coupled local motion must occur. It is important structurally that the origin (and site of the sulphate ion) is a crystallographic centre of symmetry, implying an intrinsic disorder for the non-centrosymmetric SO_4^{2-} ions. We must be clear, however, that diffraction studies of the present type will not provide local information—either about the static or the dynamical properties of the implied local ordering phenomena (the structural picture obtained is only a space-time average). Quasi-elastic diffuse neutron scattering may well supply this information; such measurements have been carried out and the data are currently under analysis.

Let us now consider the extra information the present more extensive data set adds to our picture of the structure of the high-temperature phase of Li_2SO_4. The new model, which is summarized in table 1, contains the following qualitative features:

(i) The nuclear density associated with each SO_4^{2-} ion is seen to have a centrosymmetric distortion. Although the refinement procedure is unable to resolve the effect, the Fourier sum suggests that anions (themselves non-centrosymmetric) have preferred S–O directions in the stucture. Figure 2(*b*) indicates that the oxygen atoms appear to occupy 48 h-positions (*Fm3m* notation) of type $(0, x, x)$, $(0, x, -x)$, $(0, -x, -x)$,

$(0, -x, x)$; $(x, 0, x)$, etc for $x \simeq 0.16$; 12 positions in all. We note, however, that the apparent O positions are not consistent with the tetrahedral symmetry of a SO_4 group. The angles between the 48 h positions are 60°, 90° or 120° apart, and not as in the regular SO_4^{2-} tetrahedron: 109.47°. A more plausible explanation for the apparent peaks in the oxygen distribution is that they, in fact, portray a time-averaged overlap of (positive scattering length) O nuclei and (negative scattering length) Li nuclei. Regions of apparent O depletion (typically at $Z(0, 0, 0.18)$ in figure 2(*b*)) indicate where Li nuclei reside, and thus give strong support to a paddle-wheel type Li^+ transport mechanism. Indeed, it is consistent with this picture that these peaks could not be refined explicitly as O atoms in a structural model. The combined (interlocking) Li and SO_4 distribution is described well by the refined model (table 1); as confirmed by the featureless character of the final residue maps given in figure 3.

(ii) Roughly 90% of the Li^+ ions occupy $(\frac{1}{4}, \frac{1}{4}, \frac{1}{4})$ or one of the seven other symmetry-related 8c-sites in the FCC cell. The average distribution for each Li^+ ion is significantly tetrahedrally distorted in the four (tetrahedrally related) directions towards $(0, 0, 0)$, $(\frac{1}{2}, \frac{1}{2}, 0)$, $(\frac{1}{2}, 0, \frac{1}{2})$ and $(0, \frac{1}{2}, \frac{1}{2})$ (figures 1 and 4). It is significant that the tetrahedral Li^+ displacement brings each Li^+ ion to within $\simeq 2.8$ Å of the central S atom belonging to its nearest-neighbour SO_4^{2-} ion. This figure (2.8 Å) is exactly that found for the radius of the Li^+ shell. Such local lithium relaxations into the sphere occupied by the SO_4^{2-} ions can, of course, only occur when the sulphate oxygens are themselves not occupying these regions. This picture implies a total of 32 (i.e. 8×4) possible Li sites per cell (typically, points P and Q in figure 2(*b*)), each with a mean occupation of 22–23%. The remaining 10% of the Li^+ ions (a figure arrived at by a painstaking sequence of iterations) lie on the 2.8 Å radius shell surrounding the SO_4^{2-} anions. It is clearly suggested that this feature can be related to the contribution from the mobile Li^+ ions. A Li^+ ion at one of four sites displaced from $(\frac{1}{4}, \frac{1}{4}, \frac{1}{4})$ will have six symmetry equivalent (90%-occupied) Li^+-sites to jump to; one such position (Q) is seen in figure 2(*b*) near $(\frac{3}{4}, \frac{3}{4}, \frac{1}{4})$. This means that, of the eight Li^+ ions/cell, 0.8 (i.e. roughly one) must be mobile at any one time, and that each 'stationary' Li^+ ion, near $[\frac{1}{4}, \frac{1}{4}, \frac{1}{4}]$), has approximately a 60% chance of having a vacant Li^+ site to move to (see figure 1). This would seem (in qualitative terms) a highly favourable set of conditions for an efficient transfer of Li^+ ions.

4.1. The lithium transport mechanism

Three possible Li^+ transport pathways (A, B and C) are indicated in figure 2(*b*). It has been stated earlier, however, that no lithium occupation could be refined at or near the octahedral site at $(\frac{1}{2}, \frac{1}{2}, \frac{1}{2})$; suggesting that this region does not serve as a 'resting place' for lithium ions (path A), as has often been suggested. Neither would it seem that the lithium transfer mechanism can involve hops between adjacent Li sites along axial directions (path B): the Li^+ distribution does not extent in these directions. Rather, on the basis of the refined model and the features appearing in the Fourier synthesis maps (Li^+ intrusion into the SO_4 sphere at positions avoided by the S–O bond vectors), the Li^+ transport appears to occur along a pathway of continuous lithium occupation (path C) involving the distorted lithium positions at typically $P(\frac{1}{4} + \delta, \frac{1}{4} + \delta, \frac{1}{4} - \delta)$, and a region of 'mobile' lithium occupation midway between P and Q, which depletes the apparent O density at these positions. The lithiums move through this region to positions from which they can again move into displaced (tetrahedrally distorted) Li sites; typically Q at $(\frac{3}{4} - \delta, \frac{3}{4} - \delta, \frac{1}{4} - \delta)$. It should be noted that the distance between points P and Q in figure 2(*b*) is $\simeq 3.7$ Å, and would correspond to jumps between displaced Li sites along

the [110] direction. This agrees perfectly with the value of 3.7 ± 0.4 Å obtained from Raman spectroscopy (Aronsson *et al* 1983). Diffuse neutron scattering studies also supports this jump-mode: Li–Li pair correlation distances of 3.6–3.7 Å were observed (Nilsson 1981). Although path B is also ≈3.5 Å, we have discounted it for the reasons given above.

We see that, although the above discussion involves some measure of speculation, it remains abundantly clear that this new experiment lends convincing support to our earlier naive picture of lithium movement through a 'paddle-wheel mechanism', and adds a new level of structural sophistication.

Finally, we should comment on the extensive molecular dynamics (MD) simulation of the high-temperature phase of Li_2SO_4 made by Impey *et al* (1985). This was an attempt to establish the existence of some form of coupling between reorientation of SO_4^{2-} ions and Li^+ jumps—indeed, to obtain evidence for a 'paddle-wheel mechanism'. It was found that no definite conclusions could be drawn: the scarcity of 'successful jumps' during the course of the simulation made it impossible to make a statistically valid analysis of the mechanism. There was some indication, however, of curved Li^+ pathways; which would again support the suggestion of the pathways of type C, as indicated in figure 2(*b*).

Acknowledgments

We hereby gratefully acknowledge support for this work from The Swedish Natural Science Research Council (NFR). One of us (NHA) is also indebted to The Danish Ministry of Energy for financial support.

References

Aronsson R, Börjesson L and Torell L M 1983 *Phys. Lett.* **98A** 205–7
Aronsson R, Knape H E G , Lundén A, Nilsson L, Torell L M, Andersen N H and Kjems J K 1983 *Radiat. Eff.* **75** 79–84
Bachmann R and Schulz H 1984 *Acta Crystallogr.* A **40** 668–675
Dissanayake M A K L and Mellander B-E 1986 *Solid State Ion.* **21** 279–85
Førland T and Krogh-Moe J 1957 *Acta Chem. Scand.* **11** 565–567
Impey R W, Klein M L and McDonald I R 1985 *J. Chem. Phys.* **82** 4690–4698
International Tables for X-ray Crystallography 1969 vol I (Birmingham: Kynoch); 1974 vol IV
Kvist A and Lundén A 1965 *Z. Naturf.* a **20** 235–238
Lundén A 1988a *Solid State Commun.* **65** 1237–1240
—— 1988b *Solid State Ion.* **28–30** 163–167
Lundén A and Dissanayake M A K L 1991 *J. Solid State Chem.* **90** 179–184
Lundgren J-O 1982 *Report UUIC-B13-04-05* Institute of Chemistry, University of Uppsala
Mellander B-E and Nilsson L 1983 *Z. Naturf.* a **38** 1396–1399
Nilsson L 1981 *PhD Thesis* University of Gothenburg
Nilsson L, Thomas J O and Tofield B C 1980 *J. Phys. C: Solid State Phys.* **13** 6441–6451
Nord A G 1973 *Chem. Commun.* (University of Stockholm) **3**
Schroeder K, Kvist A and Ljungmark H 1972 *Z. Naturf.* a **27** 1252–1256
Secco E A 1988a *Solid State Commun.* **66** 921–923
—— 1988b *Solid State Ion.* **28–30** 168–172